nature photonics

LETTERS

PUBLISHED ONLINE: 25 OCTOBER 2009 | DOI: 10.1038/NPHOTON.2009.192

Polymer solar cells with enhanced open-circuit voltage and efficiency

Hsiang-Yu Chen[1,2], Jianhui Hou[1]*, Shaoqing Zhang[1], Yongye Liang[3], Guanwen Yang[2], Yang Yang[2], Luping Yu[3], Yue Wu[1]* and Gang Li[1]

Following the development of the bulk heterojunction[1] structure, recent years have seen a dramatic improvement in the efficiency of polymer solar cells. Maximizing the open-circuit voltage in a low-bandgap polymer is one of the critical factors towards enabling high-efficiency solar cells. Study of the relation between open-circuit voltage and the energy levels of the donor/acceptor[2] in bulk heterojunction polymer solar cells has stimulated interest in modifying the open-circuit voltage by tuning the energy levels of polymers[3]. Here, we show that the open-circuit voltage of polymer solar cells constructed based on the structure of a low-bandgap polymer, PBDTTT[4], can be tuned, step by step, using different functional groups, to achieve values as high as 0.76 V. This increased open-circuit voltage combined with a high short-circuit current density results in a polymer solar cell with a power conversion efficiency as high as 6.77%, as certified by the National Renewable Energy Laboratory.

Polymer solar cells (PSCs) have attracted much attention due to their potential in low-cost solar energy harvesting, as well as applications in flexible, light-weight, colourful and large-area devices. With the discovery of efficient photo-induced electron transfer from a conjugated polymer to fullerene[1], the bulk heterojunction (BHJ) PSC has become one of the most successful device structures developed in the field to date. By simply blending polymers (electron donors) with fullerene (electron acceptor) in organic solvents, a self-assembling interpenetrating network can be obtained using various coating technologies ranging from laboratory-scale spin coating or spray coating to large-scale fabrication technologies such as inkjet printing[5,6], doctor blading[2], gravure[7], slot-die coating[8] and flexographic printing[9]. In the last few years, several effective methods have been developed to optimize the interpenetrating network formed by the electron donor and acceptor, including solvent annealing (or slow-growth)[10], thermal annealing[11–13] and morphology control using mixed solvent mixtures[14] or additives[15] in the solutions of donor/acceptor blends. Poly(3-hexylthiophene) (P3HT) in particular has been subject to increasing interest in the polymer research community, but significant progress has also been made in developing new active-layer polymer materials[4,15–22]. Since around 2008, the efficiency of PSCs has risen to ~6% using new conjugated polymers as electron donors[19]. Although progress has been impressive, there is still much to do before the realization of practical applications of PSCs. Many factors need to be taken into account in efficiently converting sunlight into electricity. The absorption range, the photon–electron conversion rate and the carrier mobilities of the light-harvesting polymers are among the crucial parameters for achieving high-efficiency solar cells. Furthermore, fabricating large-area devices without significantly losing efficiency while maintaining long device lifetimes remains challenging[23].

In principle, the strategies used to improve BHJ solar cell efficiency include (i) reducing the bandgap of polymers so as to harvest more sunlight, which leads to higher short-circuit current density (J_{sc}) and (ii) lowering the highest occupied molecular orbital (HOMO) of the polymers, which increases the open-circuit voltage (V_{oc}). With the rise in interest in using low-bandgap polymers to harvest more sunlight from longer wavelengths, much effort has been made recently in reducing the bandgap of polymers. Others[4,15,21] have reported PSCs with power conversion efficiencies (PCE) of over 5% using different low-bandgap polymers. The extended absorption of sunlight at longer wavelengths directly reflects on the value of J_{sc}, and a current density of up to 16 mA cm^{-2} has been achieved[15]. On the other hand, PSCs with high V_{oc} have been realized by other groups[19,20,22] by using polymers that absorb at shorter wavelengths. To push the PCE of PSCs towards the predicted theoretical limitation[24], however, achieving both a high J_{sc} and a high V_{oc} is critical, indeed essential. To match the energy level of the commonly used electron acceptor [6,6]-phenyl-C_{61}-butyric acid methyl ester (PCBM), both the HOMO and the lowest unoccupied molecular orbital (LUMO) of the polymer need to be considered while tuning the bandgap of polymers. It is known that the energy difference between the LUMOs of donor and acceptor should be larger than 0.3 eV for efficient charge separation[24], which directly relates to the J_{sc} of solar cells. However, the V_{oc} of PSCs is limited by the difference between the HOMO of the donor and the LUMO of the acceptor[2]. As a result, narrowing the bandgap of polymers without sacrificing efficient charge separation as well as high V_{oc} becomes a major hurdle in achieving high-efficiency PSCs. In this work, we attempt to alter the HOMO of poly[4,8-bis-substituted-benzo [1,2-b:4,5-b′]dithiophene-2,6-diyl-alt-4-substituted-thieno[3, 4-b]thiophene-2,6-diyl] (PBDTTT)-derived polymers[4] by adding different electron-withdrawing functional groups, step by step. We have shown that the addition of more than one electron-withdrawing group is effective in further lowering the HOMO of PBDTTT.

As reported, PSCs based on the copolymer of benzo[1,2-b:4,5-b′]dithiophene and thieno[3,4-b]thiophene (ref. 4) (hereafter referred to as PBDTTT–E, Fig. 1) can yield a J_{sc} greater than 15 mA cm^{-2} with a V_{oc} of ~0.6 V. We chose this polymer system and tried to increase PSC performance by increasing the V_{oc} through molecular design. Previous studies on thiophene-based polymers have shown that the alkyloxy chain has a much stronger electron-donating effect than an alkyl chain[25]. As a result, the HOMO of poly(3-alkoxythiophene) is higher than that of poly(3-alkylthiophene). Based on this knowledge, we replaced the alkyloxy group on the carbonyl of the thieno[3,4-b]thiophene unit with an alkyl side chain (hereafter referred to as PBDTTT–C). Both

[1]Solarmer Energy Inc., El Monte, California 91731, USA, [2]Department of Materials Science and Engineering, University of California, Los Angeles, Los Angeles, California 90095, USA, [3]Department of Chemistry and the James Franck Institute, The University of Chicago, 929 East 57th Street, Chicago, Illinois 60637, USA. *e-mail: jianhuih@solarmer.com; yuew@solarmer.com

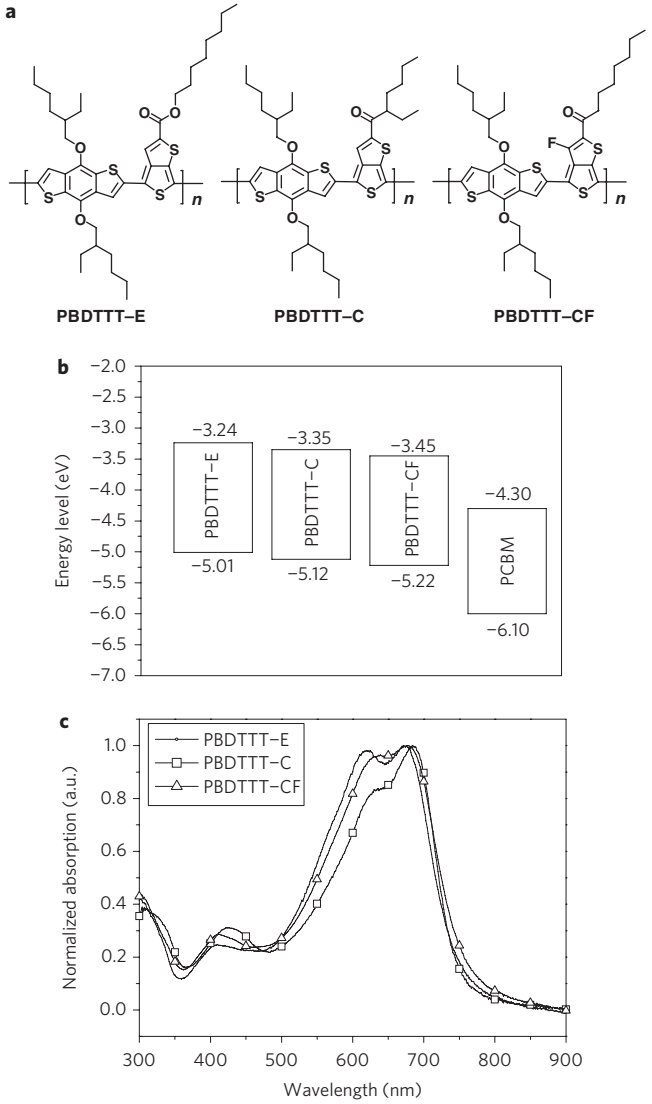

Figure 1 | Comparison of three different polymers. a–c, Chemical structure (**a**), energy levels (**b**) and absorption spectra (**c**) of PBDTTT-E, PBDTTT-C and PBDTTT-CF. Different HOMOs and LUMOs were obtained when different functional groups were attached to the PBDTTT backbone. Nevertheless, the absorption edges of these three polymers are about the same.

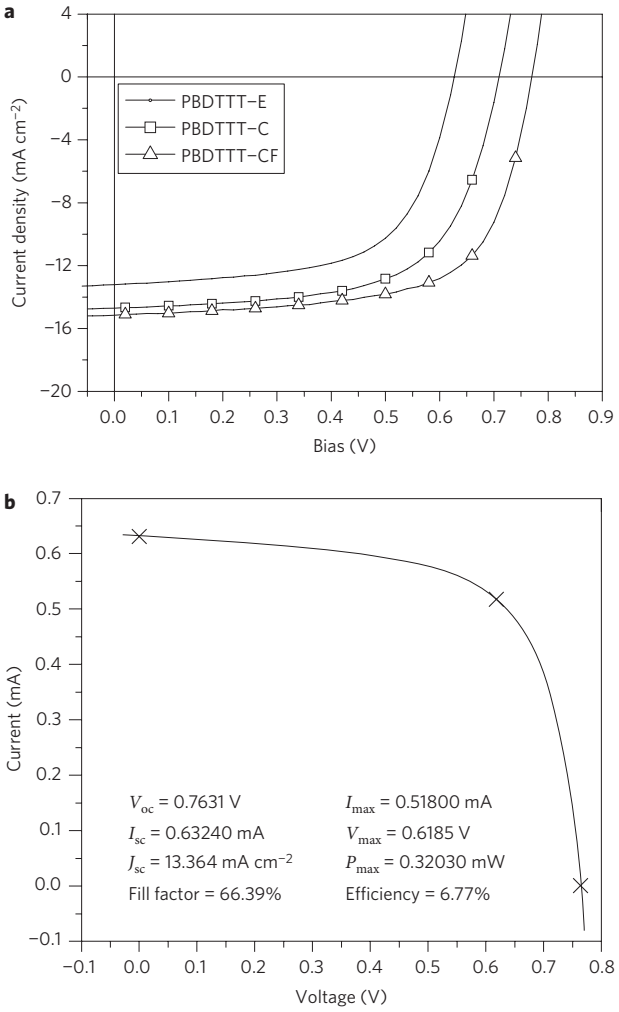

Figure 2 | Characterization of devices based on PBDTTT-E, PBDTTT-C and PBDTTT-CF. a, Current density versus voltage (J–V) curves obtained from our laboratory. **b**, J–V curve of a device based on PBDTTT-CF certified by the NREL. A significant increase in the open-circuit voltage (V_{oc}) is clearly seen between the PBDTTT-E and PBDTTT-CF. A V_{oc} of up to 0.76 V was observed in devices based on PBDTTT-CF.

PBDTTT–E and PBDTTT–C (Fig. 1a) were thus synthesized and their HOMO and LUMO levels measured by means of electrochemical cyclic voltammetry (CV). Lower HOMO and LUMO levels were observed for PBDTTT–C than for PBDTTT–E, as shown in Fig. 1b. Interestingly, the alkyl group not only results in a lower HOMO but also a lower LUMO; both the HOMO and the LUMO of PBDTTT–C are ~0.1 eV lower than those of PBDTTT–E. Therefore, the bandgap of PBDTTT–C is approximately the same as that of PBDTTT–E, which is supported by their absorption spectra (Fig. 1c).

In addition to grafting side chains, substitution of the carbon atom in selected locations also affects the energy levels of a polymer. In the recent work[26], higher values of V_{oc} are observed when fluorine, an atom of high electron affinity, is introduced to the thieno[3,4-b]thiophene unit, a PCE of 6.1% having been demonstrated[26]. To this end, PBDTTT–C was modified with a fluorine atom to lower its HOMO level. The structure of the designed and synthesized PBDTTT–CF is shown in Fig. 1a. The HOMO and LUMO of PBDTTT–CF were measured and compared with PBDTTT–C (Fig. 1b). As was observed with the addition of the alkyl group, the introduction of fluorine further lowered both the HOMO and LUMO levels. It is rather interesting that the HOMO and LUMO of this polymer system have this peculiar property. It is known that the application of a functional group to a polymer backbone causes either the HOMO or LUMO level to shift. However, to our knowledge, a change in both the HOMO and LUMO levels with just one synthetic modification to the polymer backbone has not been reported in any polymer system. The reason for this simultaneous change is not clear and is still under investigation. The absorption spectra of polymer films based on these three polymers show similar absorption edges (at ~770 nm), suggesting similar bandgaps. This is consistent with the CV results.

PSC devices based on these three polymers were fabricated and tested under simulated 100 mW cm^{-2} AM1.5G illumination (see Methods). The optimized weight ratios of polymer to $PC_{70}BM$ for PBDTTT–E, PBDTTT–C and PBDTTT–CF are 1:1, 1:1.5 and 1:1.5, respectively. Device current density/voltage (J–V) characteristics are shown in Fig. 2a and the parameters listed in Table 1. More than 200 devices were fabricated and their highest efficiencies and average values compared to provide numerical data. From the

Table 1 | Solar cell parameters of devices based on the three different polymers.

	LUMO	HOMO	V_{oc} (V)	J_{sc} (mA cm^{-2})	FF (%)	PCE (%)	
						Best	Ave
PBDTTT-E	−3.24	−5.01	0.62	−13.2	63	5.15	4.8
PBDTTT-C	−3.35	−5.12	0.7	−14.7	64.1	6.58	6.3
PBDTTT-CF	−3.45	−5.22	0.76	−15.2	66.9	7.73	7.4

LUMO, lowest unoccupied molecular orbital; HOMO, highest occupied molecular orbital; FF, fill factor, PCE, power conversion efficiency.

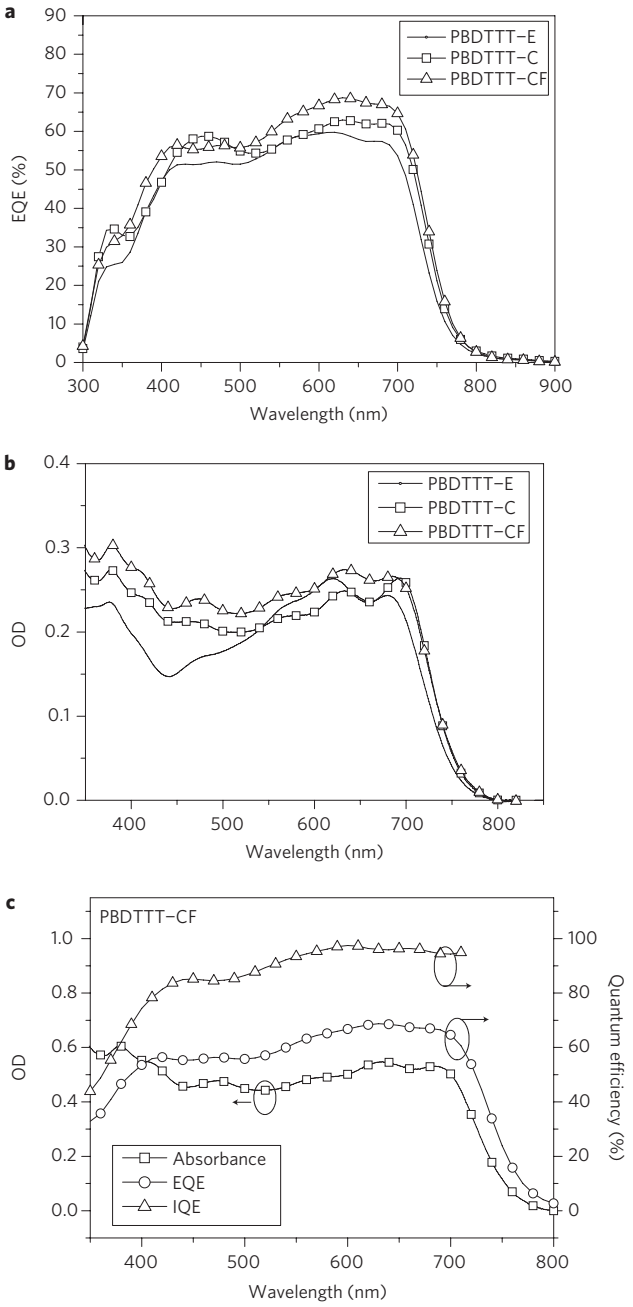

Figure 3 | Photoconversion efficiency study. a–c, External quantum efficiency (EQE) (**a**) and absorption (OD, optical density) (**b**) for devices based on PBDTTT-E, PBDTTT-C and PBDTTT-CF, and internal quantum efficiency (IQE) for device based on PBDTTT-CF (**c**). The average IQE is greater than 90% in the range 400–700 nm. Near 100% IQE was obtained for the device based on PBDTTT-CF, indicating a highly efficient overall photoconversion process in the cell.

J–V curves, a significant increase in V_{oc} is clearly observed from PBDTTT–E to PBDTTT–CF. A V_{oc} as high as 0.76 V was observed in devices based on PBDTTT–CF. Combined with its high J_{sc} and fill factor (FF), a high PCE of 7.38±0.4% (a 5% device variation), measured in more than 75 devices, was achieved in the PBDTTT–CF system, the highest measured PCE being 7.73%. Devices were then encapsulated and sent to the National Renewable Energy Laboratory (NREL) for certification. A certified efficiency of 6.77% (the highest efficiency achieved so far for organic solar cells) was rated, which differs by ∼8% from the average obtained efficiency of 7.38%. The current/voltage curve and corresponding parameters are shown in Fig. 2b. Among the parameters, the drop in efficiency results predominantly from the lower J_{sc}, most probably due to degradation of the device[27]. Although the devices were encapsulated with UV epoxy before shipping to NREL, this non-ideal encapsulation process has been observed to cause an efficiency drop of ∼3% over a 10-day storage period in a nitrogen-filled glovebox (<0.1 ppm O_2 and H_2O). Furthermore, part of the device metal finger (non-active area) was exposed to air during wiring for measurement purposes. Oxidation of the calcium/aluminium electrodes when exposed to air could also contribute to this difference.

To further confirm the accuracy of the measurements, the external quantum efficiency (EQE) of the devices based on the three polymers was measured using an EQE system (Model QEX7) purchased from PV Measurements. The EQE curves are shown in Fig. 3a. All the devices show rather efficient photoconversion efficiency in the range 400–700 nm, with EQE values of 50–70%. In the PBDTTT–CF device, the highest EQE value was 68.7% at 630 nm, which, to the best of our knowledge, is the highest achieved in a low-bandgap PSCs system. The J_{sc} values were then calculated by integrating the EQE data with an AM1.5G reference spectrum. The calculated J_{sc} values were −13.0, −14.1 and −15.0 mA cm^{-2} for devices based on PBDTTT–E, PBDTTT–C and PBDTTT–CF, respectively. These values are rather consistent with those (within 4% error, see Table 1) obtained from the *J–V* measurement. In fact, the J_{sc} values for the PBDTTT–CF solar cell obtained using these two methods are rather close (−15.0 and −15.2 mA cm^{-2}, ∼1% difference). The absorption curves of polymer:$PC_{70}BM$ blend films are shown in Fig. 3b. Significant absorption increases are observed in the absorption range 300–600 nm after blending with $PC_{70}BM$. According to the absorption spectrum, the polymer films still have ∼50% transparency (optical density, OD ≈ 0.3) under optimized device conditions, suggesting their potential as a material for tandem or stackable solar cells[28]. The internal quantum efficiency (IQE) of the device based on PBDTTT–CF was obtained from its absorption spectrum and EQE curve. As shown in Fig. 3c, the average IQE was higher than 90% in the range 400–700 nm, indicating a highly efficient overall photoconversion process in the cell. To reach such a high IQE, it is necessary to simultaneously achieve efficient light absorption, exciton diffusion, charge separation and carrier collection. Physically, this indicates a close to ideal polymer active layer morphology, with a bicontinuous interpenetrating polymer/fullerene network. Combined with the high V_{oc} and FF, a solar cell with efficiency greater than 7% was achieved. The carrier mobilities of these three devices were measured using the space charge

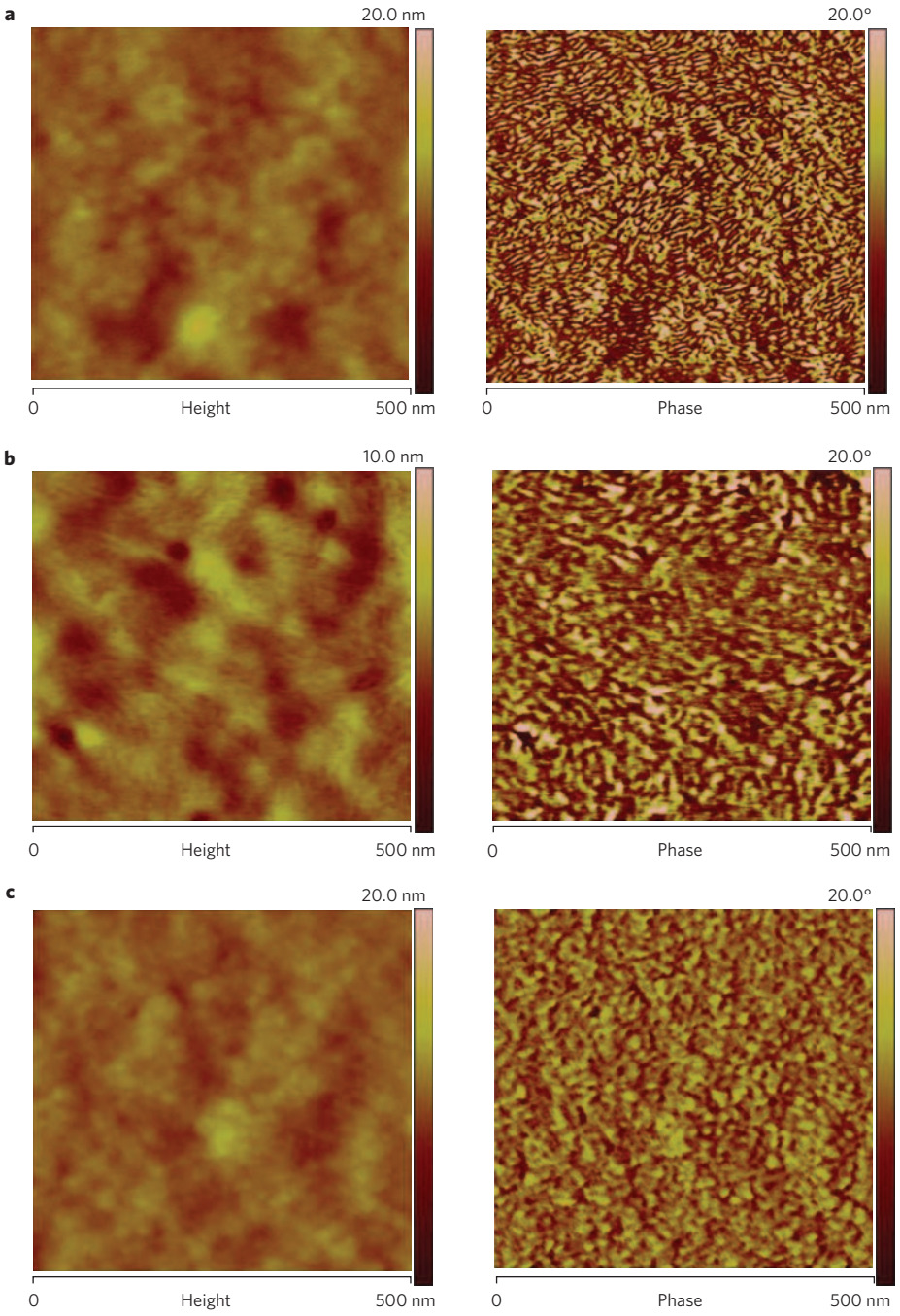

Figure 4 | Tapping-mode atomic force microscopy images of the three films used in making the devices (under optimized device conditions). **a**–**c**, The topography of each film is shown in the left panels, and the corresponding phase images in the right panels. Very different surface morphologies were obtained for the different polymer films. Fibrillar features are clearly seen in PBDTTT-E (**a**) and PBDTTT-C (**b**) films, whereas domains with different shapes are observed in the PBDTTT-CF (**c**) film. The fibrillar features can be clearly seen even in the topography image of the PBDTTT-C film.

limited current (SCLC) method reported previously[29]. The hole mobilities obtained using this method were $\sim 4 \times 10^{-4}$, 2×10^{-4} and 7×10^{-4} $cm^2\ V^{-1}\ s^{-1}$ for PBDTTT–E, PBDTTT–C and PBDTTT–CF devices, respectively. The observed variation in the hole mobilities of these three polymers may be the reason for the difference in thickness existing in the optimized devices (~790, 660 and 970 Å, respectively).

The nanoscale morphologies of the polymer/$PC_{70}BM$ films were studied using tapping-mode atomic force microscopy (AFM). Surface topography (left) and phase images (right) were taken for each film and are shown in Fig. 4. Surface roughness values measured from the topography images were ~0.96, 0.92 and 0.84 nm for PBDTTT–E (Fig. 4a), PBDTTT–C (Fig. 4b) and PBDTTT–CF (Fig. 4c) films, respectively. Very different morphologies were observed for these three polymers in their phase images (Fig. 4, right panels). As shown in Fig. 4, fibrillar features are clearly seen in PBDTTT–E (Fig. 4a) and PBDTTT–C (Fig. 4b) films, whereas domains with different shapes are observed in the PBDTTT–CF (Fig. 4c) film. Fibrillar features can be clearly seen even in the topography image of the PBDTTT–C film. The very different morphology of these three polymer films suggests that the interactions between the molecules of each polymer may be different. The fact that the polymer system (PBDTTT–CF) with seemingly lowest organization shows the highest performance differs

greatly from the widely studied benchmark P3HT solar cell system[30,31], in which the noodle-like structure typically correlates very well to the crystallinity[32] as well as the PCE. This indicates that the correlation of the morphology and PCE in the new polymer systems differs significantly from conventional understanding. Further investigation is under way to provide more information.

To conclude, tuning the V_{oc} of PSCs by means of molecular design has been realized using a step-by-step approach. Applying stronger electron-withdrawing groups to the backbone of polymers has been found to be effective in lowering the HOMO of polymers, which directly affects the V_{oc} of PSCs. Based on the PBDTTT polymer derivative system, PSCs with a PCE higher than 7% have been realized by combining the advantages of a low HOMO level in the polymer (high V_{oc}) and long wavelength absorption (high J_{sc}). Regarding the LUMO level of PCBM, there is still much capacity for increasing the V_{oc} by tuning the energy levels of the polymers. A further improvement in efficiency can be expected if the HOMO of the polymer can be further lowered without loss of J_{sc}.

Methods

All the polymers were synthesized in our laboratory and $PC_{70}BM$ was purchased from Nano-C (used as received). Polymers and $PC_{70}BM$ were then dissolved in chlorobenzene with 1:1 (PBDTTT–E:$PC_{70}BM$ = 10 mg ml^{-1}:10 mg ml^{-1}) and 1:1.5 (10 mg ml^{-1}:15 mg ml^{-1}) weight ratio, respectively. 1,8-Diiodooctane (purchased from Sigma Aldrich, used as received) with 3% volume ratio was then added to the solutions and stirred before use. The solutions were spin-coated on indium tin oxide (ITO)/glass substrates with a pre-coated PEDOT:PSS (poly(ethylenedioxythiophene):polystyrene sulphonate) layer. The device active area was ~0.1 cm^2 for all the solar cell devices discussed in this work. Device characterization was carried out in air after encapsulation under simulated AM1.5G irradiation (100 mW cm^{-2}) using a xenon-lamp-based solar simulator. EQE measurements of the encapsulated devices were performed in air (PV Measurements, Model QEX7). Some oxidization of the electrodes (calcium/aluminium) was observed when the devices were open to the air.

Received 3 August 2009; accepted 28 September 2009; published online 25 October 2009

References

1. Sariciftci, N. S., Smilowitz, L., Heeger, A. J. & Wudl, F. Photoinduced electron-transfer from a conducting polymer to buckminsterfullerene. *Science* **258,** 1474–1476 (1992).
2. Brabec, C. J. *et al.* Origin of the open circuit voltage of plastic solar cells. *Adv. Funct. Mater.* **11,** 374–380 (2001).
3. Hou, J. H. *et al.* Bandgap and molecular energy level control of conjugated polymer photovoltaic materials based on benzo[1,2-b:4,5-b']dithiophene. *Macromolecules* **41,** 6012–6018 (2008).
4. Liang, Y. Y. *et al.* Development of new semiconducting polymers for high performance solar cells. *J. Am. Chem. Soc.* **131,** 56–57 (2009).
5. Hoth, C. N., Choulis, S. A., Schilinsky, P. & Brabec, C. J. High photovoltaic performance of inkjet printed polymer: fullerene blends. *Adv. Mater.* **19,** 3973–3978 (2007).
6. Aernouts, T., Aleksandrov, T., Girotto, C., Genoe, J. & Poortmans, J. Polymer based organic solar cells using ink-jet printed active layers. *Appl. Phys. Lett.* **92,** 033306 (2008).
7. Pudas, M., Hagberg, J. & Leppavuori, S. Gravure offset printing of polymer inks for conductors. *Progr. Org. Coatings* **49,** 324–335 (2004).
8. Krebs, F. C., Gevorgyan, S. A. & Alstrup, J. A roll-to-roll process to flexible polymer solar cells: model studies, manufacture and operational stability studies. *J. Mater. Chem.* **19,** 5442–5451 (2009).
9. Krebs, F. C. Fabrication and processing of polymer solar cells: a review of printing and coating techniques. *Sol. Eng. Mater. Sol. Cells* **93,** 394–412 (2009).
10. Li, G. *et al.* High-efficiency solution processable polymer photovoltaic cells by self-organization of polymer blends. *Nature Mater.* **4,** 864–868 (2005).
11. Ma, W. L., Yang, C. Y., Gong, X., Lee, K. & Heeger, A. J. Thermally stable, efficient polymer solar cells with nanoscale control of the interpenetrating network morphology. *Adv. Funct. Mater.* **15,** 1617–1622 (2005).
12. Padinger, F., Rittberger, R. S. & Sariciftci, N. S. Effects of postproduction treatment on plastic solar cells. *Adv. Funct. Mater.* **13,** 85–88 (2003).
13. Li, G., Shrotriya, V., Yao, Y. & Yang, Y. Investigation of annealing effects and film thickness dependence of polymer solar cells based on poly(3-hexylthiophene). *J. Appl. Phys.* **98,** 043704 (2005).
14. Zhang, F. L. *et al.* Influence of solvent mixing on the morphology and performance of solar cells based on polyfluorene copolymer/fullerene blends. *Adv. Funct. Mater.* **16,** 667–674 (2006).
15. Peet, J. *et al.* Efficiency enhancement in low-bandgap polymer solar cells by processing with alkane dithiols. *Nature Mater.* **6,** 497–500 (2007).
16. Chen, C. P., Chan, S. H., Chao, T. C., Ting, C. & Ko, B. T. Low-bandgap poly(thiophene–phenylene–thiophene) derivatives with broaden absorption spectra for use in high-performance bulk-heterojunction polymer solar cells. *J. Am. Chem. Soc.* **130,** 12828–12833 (2008).
17. Blouin, N., Michaud, A. & Leclerc, M. A low-bandgap poly(2,7-carbazole) derivative for use in high-performance solar cells. *Adv. Mater.* **19,** 2295–2300 (2007).
18. Gadisa, A. *et al.* A new donor–acceptor–donor polyfluorene copolymer with balanced electron and hole mobility. *Adv. Funct. Mater.* **17,** 3836–3842 (2007).
19. Park, S. H. *et al.* Bulk heterojunction solar cells with internal quantum efficiency approaching 100%. *Nature Photon.* **3,** 297–303 (2009).
20. Chen, M. H. *et al.* Efficient polymer solar cells with thin active layers based on alternating polyfluorene copolymer/fullerene bulk heterojunctions. *Adv. Mater.* **21,** 1–5 (2009).
21. Hou, J., Chen, H.-Y., Zhang, S., Li, G. & Yang, Y. Synthesis, characterization and photovoltaic properties of a low bandgap polymer based on silole-containing polythiophenes and benzo[c][1,2,5]thiadiazole. *J. Am. Chem. Soc.* **130,** 16144–16145 (2008).
22. Wang, E. *et al.* High-performance polymer heterojunction solar cells of a polysilafluorene derivative. *Appl. Phys. Lett.* **92,** 033307 (2008).
23. Krebs, F. C. *et al.* A complete process for production of flexible large area polymer solar cells entirely using screen printing—first public demonstration. *Sol. Eng. Mater. Sol. Cells* **93,** 422–441 (2009).
24. Scharber, M. C. *et al.* Design rules for donors in bulk-heterojunction solar cells—towards 10% energy-conversion efficiency. *Adv. Mater.* **18,** 789–794 (2006).
25. Shi, C. J., Yao, Y., Yang, Y. & Pei, Q. B. Regioregular copolymers of 3-alkoxythiophene and their photovoltaic application. *J. Am. Chem. Soc.* **128,** 8980–8986 (2006).
26. Liang, Y. Y. *et al.* Highly efficient solar cell polymers developed via fine-tuning of structural and electronic properties. *J. Am. Chem. Soc.* **131,** 7792–7799 (2009).
27. Jorgensen, M., Norrman, K. & Krebs, F. C. Stability/degradation of polymer solar cells. *Sol. Eng. Mater. Sol. Cells* **92,** 686–714 (2008).
28. Shrotriya, V., Wu, E. H. E., Li, G., Yao, Y. & Yang, Y. Efficient light harvesting in multiple-device stacked structure for polymer solar cells. *Appl. Phys. Lett.* **88,** 064104 (2006).
29. Shrotriya, V., Yao, Y., Li, G. & Yang, Y. Effect of self-organization in polymer/fullerene bulk heterojunctions on solar cell performance. *Appl. Phys. Lett.* **89,** 063505 (2006).
30. Li, G. *et al.* 'Solvent annealing' effect in polymer solar cells based on poly(3-hexylthiophene) and methanofullerenes. *Adv. Funct. Mater.* **17,** 1636–1644 (2007).
31. Li, G., Shrotriya, V., Yao, Y., Huang, J. S. & Yang, Y. Manipulating regioregular poly(3-hexylthiophene): [6,6]-phenyl-C-61-butyric acid methyl ester blends—route towards high efficiency polymer solar cells. *J. Mater. Chem.* **17,** 3126–3140 (2007).
32. Chu, C. W. *et al.* Control of the nanoscale crystallinity and phase separation in polymer solar cells. *Appl. Phys. Lett.* **92,** 103306 (2008).

Acknowledgements

The National Renewable Energy Laboratory (NREL) is thanked for conducting the certification of devices. The authors in particular thank D.C. Olson at NREL for his help in verifying and certifying the performances of our devices.

Author contributions

H.Y.C. conceived and performed PSC fabrication, measurements and data analysis. Y.L. and L.Y. contributed to the design of the polymer's main chain structure. J.H. designed the polymer structures and synthesis routes. S.Z. synthesized the polymers. G.Y. performed the AFM image scans. J.H. and Y.W. conceptualized and directed the research project. All authors discussed the results and commented on the manuscript.

Additional information

Reprints and permission information is available online at http://npg.nature.com/reprintsandpermissions/. Correspondence and requests for materials should be addressed to J.H. and Y.W.